

Synthesis and Characterization of Ethylbis(2-pyridylethyl)amineruthenium Complexes and Two Different Types of C–H Bond Cleavage at an Ethylene Arm

Sohei Fukui,[†] Akari Kajihara,[†] Toshiyuki Hirano,[‡] Fumitoshi Sato,[‡] Noriyuki Suzuki,[†] and Hirotaka Nagao^{*,†}

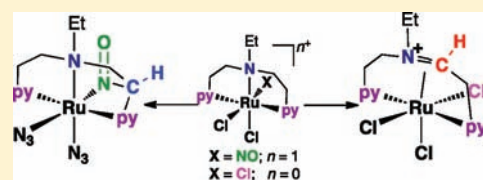
[†]Department of Materials and Life Sciences, Faculty of Science and Technology, Sophia University, 7-1 Kioicho, Chiyoda-ku, Tokyo, 102-8554 Japan

[‡]Institute of Industrial Science, The University of Tokyo, 4-6-1 Komaba, Meguro-ku, Tokyo 153-8505, Japan

S Supporting Information

ABSTRACT: Ruthenium complexes bearing ethylbis(2-pyridylethyl)amine (ebpea), which has flexible $-C_2H_4-$ arms between the amine and the pyridyl groups and coordinates to a metal center in facial and meridional modes, have been synthesized and characterized. Three trichloro complexes, *fac*-[Ru^{III}Cl₃(ebpea)] (*fac*-[1]), *mer*-[Ru^{III}Cl₃(ebpea)] (*mer*-[1]), and *mer*-[Ru^{II}Cl₃{ η^2 -N-(C₂H₅)(C₂H₄py)=CH-CH₂py}] (*mer*-[2]), were synthesized using the Ru blue solution. Formation of *mer*-[2] proceeded via a C–H activation of the CH₂

group next to the amine nitrogen atom of the ethylene arm. Reduction reactions of *fac*- and *mer*-[1] afforded a triacetonitrile complex *mer*-[Ru^{II}(CH₃CN)₃(ebpea)](PF₆)₂ (*mer*-[3](PF₆)₂). Five nitrosyl complexes *fac*-[RuX₂(NO)(ebpea)]PF₆ (X = Cl for *fac*-[4]PF₆; X = ONO₂ for *fac*-[5]PF₆) and *mer*-[RuXY(NO)(ebpea)]PF₆ (X = Cl, Y = Cl for *mer*-[4]PF₆; X = Cl, Y = CH₃O for *mer*-[6]PF₆; X = Cl, Y = OH for *mer*-[7]PF₆) were synthesized and characterized by X-ray crystallography. A reaction of *mer*-[2] in H₂O–C₂H₅OH at room temperature afforded *mer*-[1]. Oxidation of C₂H₅OH in H₂O–C₂H₅OH and *i*-C₃H₇OH in H₂O–*i*-C₃H₇OH to acetaldehyde and acetone by *mer*-[2] under stirring at room temperature occurred with formation of *mer*-[1]. Alternative C–H activation of the CH₂ group occurred next to the pyridyl group, and formation of a C–N bond between the CH moiety and the nitrosyl ligand afforded a nitroso complex [Ru^{II}(N₃)₂{N(O)CH(py)CH₂N(C₂H₅)C₂H₄py}] ([8]) in reactions of nitrosyl complexes with sodium azide in methanol, and reaction of [8] with hydrochloric acid afforded a corresponding chloronitroso complex [Ru^{II}Cl₂{N(O)CH(py)CH₂N(C₂H₅)C₂H₄py}] ([9]).



INTRODUCTION

Ruthenium complexes bearing pyridyl-containing supporting ligands such as 2,2′-bipyridine (bpy) have been investigated on their photo- and electrochemical behavior.¹ These behaviors relate to their function as catalysts and mediators for electron and energy transfer. Ruthenium complexes containing tridentate 2,2′:6′,2′′-terpyridine (trpy), which has a wide π -conjugated system and π -accepting nature, have been used in studies on photochemical and electrochemical properties as well as (2,2′-bipyridine)ruthenium complexes.² Alternate tridentate ligands containing pyridine ring(s) and alkyl chains, alkylphosphine-based pincer ligand PNP and PNN and pyridylalkylamine ligand, have been used as supporting ligand and catalyst for conversion of substrates such as alcohols, amines, carbon dioxide, and esters.³ Bis(pyridylalkyl)amine tridentate ligands, in which one amine nitrogen atom and two pyridyl groups were connected with alkyl chains, coordinate to a metal center in both facial and meridional configurations. Ethylbis(2-pyridylmethyl)amine ($n = 1$, ebpm), which has $-CH_2-$ arms between the pyridyl and the amine groups as shown in Figure 1, has been used as a tridentate supporting ligand.

Ruthenium complexes bearing ebpm have been synthesized and investigated on their properties and structures.⁴ Their structures of the meridional complexes indicated that the ebpm

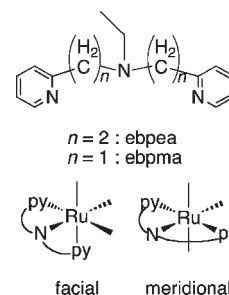


Figure 1. Bis(pyridylalkyl)amine ligands and their coordination modes.

ligand was a spatially constrained structure.⁵ In this paper, we used ethylbis(2-pyridylethyl)amine ($n = 2$, ebpea in Figure 1), having $-C_2H_4-$ arms between the amine and the pyridyl groups for investigation on syntheses of ruthenium complexes and relationships between their reactivities and geometrical configurations and synthesized ruthenium(III), ruthenium(II), and nitrosyl- and nitrosoruthenium complexes. Two different types of characteristic

Received: September 22, 2010

Published: April 25, 2011

C–H activation reactions at the alkyl chain of the ebpea ligand were found. C–H activation of the alkyl chain of ebpea occurred in the reaction of the Ru–blue solution with ebpea, and the complex functioned as a catalyst for oxidation of alcohols.⁶ C–H activation of the alkyl chain of tridentate bis(2-pyridylmethyl)amine coordinated to an iron center in a meridional form has been reported.⁷ An alternative C–H activation reaction of the –CH₂– moiety next to the pyridyl group occurred during a reaction of nitrosyl complexes to afford a nitroso complex.

EXPERIMENTAL SECTION

Measurements. IR spectra were recorded on a Perkin-Elmer FT-2000 FTIR spectrophotometer using samples prepared as KBr disks and CH₃CN solutions. Elemental analyses were carried out with a Perkin-Elmer 2400-II. ¹H and ¹³C NMR spectra were obtained with JEOL JML-AL500 and AL300 spectrometers. UV–vis spectra were obtained on a Shimadzu MultiSpec-1500 diode array spectrophotometer. Cyclic voltammetric measurements were made on CH₂Cl₂ solutions containing in 0.1 mol dm⁻³ tetra-*n*-butylammonium hexafluorophosphate (TBAH, Wako) and CH₃CN solutions in 0.1 mol dm⁻³ tetraethylammonium perchlorate (TEAP, Nakarai Tesque Ltd.) as supporting electrolyte with a platinum disk working electrode ($\phi = 1.6$ mm) and an Ag|0.01 mol dm⁻³ AgNO₃ reference electrode using a BAS 100B/W electrochemical analyzer. At the end of each measurement, ferrocene was added as an internal standard to correct redox potentials.

Materials. RuCl₃·*n*H₂O (content of Ru, 40.11 wt %) was purchased from Furuya Kinzoku Inc. K₂[RuCl₅(NO)] was prepared by a procedure reported in the literature.⁸ The ebpea ligand was prepared according to a literature procedure.⁶

Syntheses of Complexes. *fac*-[Ru^{III}Cl₃(ebpea)] (*fac*-[1]) and *mer*(Cl,Cl,Cl)-[Ru^{III}Cl₃{ η^2 -N(C₂H₅)(C₂H₄py)=CHCH₂py}] (*mer*-[2]). A dark brown solution of RuCl₃·*n*H₂O (400 mg, 1.68 mmol) in H₂O–C₂H₅OH (2:3 v/v) 40 cm³ was refluxed until the color changed to dark blue. To the magnetically stirred dark blue solution, 432 mg (1.69 mmol) of ebpea was added to give a dark green solution. The dark green solution was refluxed for 15 min.

Procedure for *fac*-[1]. To the dark green solution, 4 cm³ of hydrochloric acid was added to give a dark brown solution. The solution was refluxed for 30 min and then cooled at room temperature to give a small amount of *mer*(Cl,Cl,Cl)-[Ru^{III}Cl₃{ η^2 -N(C₂H₅)(C₂H₄py)=CHCH₂py}] (*mer*-[2]) as a dark brown precipitate. The resulting solid was removed by filtration. Then filtrate was allowed to stand at room temperature for 2 nights to give a brown precipitate that was collected by filtration and washed with H₂O, C₂H₅OH, and diethyl ether. Yield: 547 mg (73%). This complex has been characterized in the literature.⁶

Procedure for *mer*-[2]. To the dark green solution, 8 cm³ of hydrochloric acid was added to give a dark brown solution. The solution was refluxed for 30 min and then cooled at room temperature to give a dark brown precipitate that was collected by filtration and washed with H₂O, C₂H₅OH, and diethyl ether. Yield: 255 mg (42%). This complex has been characterized in the literature.⁶

mer-[Ru^{III}Cl₃(ebpea)] (*mer*-[1]). A suspended solution of *mer*-[2] (100 mg, 0.21 mmol) in CH₃OH (900 cm³) was magnetically stirred for 6 h to give a yellow solution. The volume of the yellow solution was reduced to dryness with a rotary evaporator. H₂O was added to the formed light brown solid. The complex was collected by filtration and washed with H₂O, C₂H₅OH, and diethyl ether. Yield: 72 mg (74%). This complex has been characterized in the literature.⁶

mer-[Ru^{II}(CH₃CN)₃(ebpea)](PF₆)₂ (*mer*-[3](PF₆)₂). *fac*-[1] (100 mg, 0.22 mmol) was suspended in H₂O–C₂H₅OH (1:1 v/v) 50 cm³, and CH₃CN (4 cm³) was added to the suspended solution. The mixture was refluxed for 5 h to give a light brown solution. The volume of the solution was reduced, and NH₄PF₆ (200 mg) was added as a precipitant. The

light brown product obtained was collected by filtration and washed with H₂O, C₂H₅OH, and diethyl ether. Yield: 148 mg (89%). This complex was also synthesized by *mer*-[1] instead of *fac*-[1] (80%). Anal. Calcd for C₂₂H₃₀N₆F₁₂P₂Ru: C, 34.34; H, 3.93; N, 10.92. Found: C, 34.22; H, 3.60; N, 11.07. ν (CN): 2281 cm⁻¹ (KBr). ¹H NMR (CD₃CN, 300 MHz): δ 1.24 (3H, t, *J* = 7.0 Hz, CH₃(ethyl)), 2.45 (6H, s, CH₃CN), 2.52 (3H, s, CH₃CN), 2.61–3.25 (8H, m, CH₂), 3.57 (2H, q, *J* = 7.0, CH₂(ethyl)), 7.26 (2H, ddd, *J* = 1.7, 6.0, 7.7 Hz, 5-H(py)), 7.60 (2H, d, *J* = 7.7 Hz, 3-H(py)), 8.03 (2H, td, *J* = 1.7, 7.7 Hz, 4-H(py)), 9.17 (2H, dd, *J* = 1.7, 6.0 Hz, 6-H(py)). ¹³C NMR (CD₃CN, 75.6 MHz): δ 4.64, 8.46, 35.20, 53.50, 59.08, 124.25, 126.50, 138.99, 156.45, 165.31. MS (FAB⁺): *m/z* 625 (M – PF₆).

cis, fac-[RuCl₂(NO)(ebpma)]PF₆ (*fac*-[4]PF₆). *fac*-[1] (100 mg, 0.22 mmol) was suspended in C₂H₅OH (25 cm³) containing nitric acid (60%, 1.3 cm³). The suspension was refluxed for 4 h to give a brown solution. The volume of the brown solution was reduced to dryness with a rotary evaporator. H₂O and NH₄PF₆ (120 mg) were added to the formed brown solid. The complex was collected by filtration and washed with H₂O, C₂H₅OH, and diethyl ether. Yield: 108 mg (83%). Anal. Calcd for C₁₆H₂₁N₄OF₆PCl₂Ru: C, 31.91; H, 3.51; N, 9.30. Found: C, 31.85; H, 3.29; N, 9.59. ν (NO): 1901 (KBr), 1904 cm⁻¹ (in CH₃CN). ¹H NMR (CD₃CN, 300 MHz): δ 1.38 (3H, t, *J* = 6.9 Hz, CH₃(ethyl)), 2.30 (1H, m, CH₂), 2.98 (4H, m, CH₂), 3.42 (3H, m, CH₂(ethyl) and CH₂), 3.68 (1H, m, CH₂), 4.15 (1H, m, CH₂), 7.31 (1H, ddd, *J* = 1.4, 6.5, 7.9 Hz, 5-H(py)), 7.42 (1H, d, *J* = 7.9 Hz, 3-H(py)), 7.66 (2H, m, 3-H(py) and 5-H(py)), 8.07 (3H, m, 4-H(py) and 6-H(py)), 9.88 (1H, dd, *J* = 1.4, 6.5 Hz, 6-H(py)). ¹³C NMR (CD₃CN, 75.6 MHz): δ 10.78, 33.86, 39.52, 52.92, 58.55, 63.55, 125.71, 126.01, 127.79, 128.06, 143.49, 143.56, 153.91, 154.75, 159.58, 161.12. MS (FAB⁺): *m/z* 457 (M – PF₆).

cis, mer-[RuCl₂(NO)(ebpea)]PF₆ (*mer*-[4]PF₆). K₂[RuCl₅(NO)] (100 mg, 0.26 mmol), LiCl (200 mg, 5.00 mmol), and ebpea (66 mg, 0.26 mmol) were suspended in C₂H₅OH (20 cm³). This mixture was refluxed for 3 h to give a suspended dark brown solution. After removing insoluble materials by filtration, filtrate was cooled to room temperature and NH₄PF₆ (100 mg) was added as a precipitant. The brown product obtained was collected by filtration and washed with H₂O, C₂H₅OH, and diethyl ether. Yield: 81 mg (50%). Anal. Calcd for C₁₆H₂₁N₄OF₆PCl₂Ru: C, 31.91; H, 3.51; N, 9.30. Found: C, 32.02; H, 3.32; N, 9.28. ν (NO): 1868 (KBr), 1882 cm⁻¹ (in CH₃CN). ¹H NMR (CD₃CN, 300 MHz): δ 1.03 (3H, t, *J* = 7.2 Hz, CH₃(ethyl)), 2.92 (2H, q, *J* = 7.2 Hz, CH₂(ethyl)), 3.23 (2H, m, CH₂), 3.49 (2H, m, CH₂), 3.64 (4H, t, *J* = 6.2, CH₂), 7.58 (2H, ddd, *J* = 1.7, 6.2, 7.6 Hz, 5-H(py)), 7.65 (2H, d, *J* = 7.6 Hz, 3-H(py)), 8.10 (2H, td, *J* = 1.7, 7.6 Hz, 4-H(py)), 9.41 (2H, dd, *J* = 1.7, 6.2 Hz, 6-H(py)). ¹³C NMR (CD₃CN, 75.6 MHz): δ 7.99, 35.30, 56.22, 57.82, 124.95, 128.10, 142.71, 156.48, 160.13. MS (FAB⁺): *m/z* 457 (M – PF₆).

cis, fac-[Ru(ONO)₂(NO)(ebpea)]PF₆·0.5CH₃CN (*fac*-[5]PF₆·0.5-CH₃CN). *mer*-[3](PF₆)₂ (100 mg, 0.15 mmol) was suspended in H₂O (1 cm³) with nitric acid (60%, 0.3 cm³). The suspension was refluxed for a few seconds to give a reddish brown solution. The volume of the solution was reduced, and NH₄PF₆ (200 mg) was added as a precipitant. The reddish brown product obtained was collected by filtration and washed with H₂O, C₂H₅OH, and diethyl ether. Yield: 35 mg (41%). The complex was recrystallized from CH₃CN–H₂O. Anal. Calcd for C₁₇H_{22.5}N_{6.5}O₇F₆PRu: C, 30.21; H, 3.36; N, 13.47. Found: C, 30.31; H, 3.25; N, 13.40. ν (NO): 1931 (KBr), 1931 cm⁻¹ (in CH₃CN). ¹H NMR (CD₃CN, 500 MHz): δ 1.39 (3H, t, *J* = 6.9 Hz, CH₃(ethyl)), 2.93 (2H, m, CH₂), 3.05 (1H, m, CH₂), 3.24 (1H, m, CH₂), 3.41 (2H, m, CH₂(ethyl)), 3.53 (2H, m, CH₂), 3.70 (1H, m, CH₂), 3.90 (1H, m, CH₂), 7.54 (1H, ddd, *J* = 1.4, 6.3, 7.7 Hz, 5-H(py)), 7.67 (3H, m, 3-H(py) and 5-H(py)), 8.13 (1H, td, *J* = 1.4, 7.7 Hz, 4-H(py)), 8.20 (1H, td, *J* = 1.4, 7.7 Hz, 4-H(py)), 8.23 (1H, d, *J* = 6.3 Hz, 6-H(py)), 8.72 (1H, dd, *J* = 1.4, 6.3 Hz, 6-H(py)). ¹³C NMR (CD₃CN, 126 MHz): δ 9.69, 32.94, 35.98, 54.92, 62.56, 125.70, 126.90, 128.69, 129.39,

143.50, 144.28, 150.60, 152.05, 160.71, 160.84. MS (FAB⁺): *m/z* 511 (M – PF₆).

cis,mer-[RuCl(CH₃O)(NO)(ebpea)]PF₆ (mer-[6]PF₆). Procedure A. K₂[RuCl₅(NO)] (100 mg, 0.26 mmol), NaOCH₃ (15 mg, 0.26 mmol), and ebpea (66 mg 0.26 mmol) were suspended in CH₃OH (20 cm³). This mixture was refluxed for 3 h to give a reddish brown solution. This solution was cooled to room temperature, and NH₄PF₆ (120 mg) was added and allowed to stand at room temperature for 3 nights to give a yellow precipitate that was collected by filtration and washed with H₂O, CH₃OH, and diethyl ether. Yield: 86 mg (54%). Anal. Calcd for C₁₇H₂₄N₄O₂F₆PClRu: C, 34.15; H, 4.05; N, 9.37. Found: C, 34.08; H, 3.86; N, 9.30. $\nu(\text{NO})$: 1817 (KBr), 1833 cm⁻¹ (in CH₃CN). ¹H NMR (CD₃CN, 500 MHz): δ 1.18 (3H, t, *J* = 6.9 Hz, CH₃(ethyl)), 2.82 (2H, m, CH₂), 3.28 (2H, q, *J* = 6.9 Hz, CH₂(ethyl)), 3.38 (1H, m, CH₂), 3.41 (1H, m, CH₂), 3.46 (3H, s, OCH₃), 3.81 (2H, m, CH₂), 3.88 (1H, m, CH₂), 3.91 (1H, m, CH₂), 7.48 (2H, ddd, *J* = 1.7, 6.0, 7.7 Hz, 5-H(py)), 7.60 (2H, d, *J* = 7.7 Hz, 3-H(py)), 8.03 (2H, td, *J* = 1.7, 7.7 Hz, 4-H(py)), 9.17 (2H, dd, *J* = 1.7, 6.0 Hz, 6-H(py)). ¹³C NMR (CD₃CN, 126 MHz): δ 8.78, 33.31, 53.34, 58.24, 61.67, 124.19, 128.84, 141.83, 155.62, 161.17. MS (FAB⁺): *m/z* 453 (M – PF₆).

Procedure B. mer-[4]PF₆ (50 mg, 0.083 mmol) and NaOCH₃ (5 mg, 0.093 mmol) were suspended in CH₃OH (10 cm³). This suspension was refluxed for 5 h to give an orange solution and cooled to room temperature. NH₄PF₆ (50 mg) was added as a precipitant. The brown product was collected by filtration and washed with H₂O, CH₃OH, and diethyl ether. Yield: 29 mg (59%). The obtained complex was identified as *mer-[6]PF₆* by IR spectroscopy and CV.

Procedure C. fac-[4]PF₆ (25 mg, 0.042 mmol) and NaOCH₃ (3 mg, 0.056 mmol) were suspended in CH₃OH (5 cm³). This suspension was refluxed for 3 h to give a chestnut solution, and this solution was reduced with a rotary evaporator. NH₄PF₆ (50 mg) was added as a precipitant. The brown product was collected by filtration and washed with H₂O, CH₃OH, and diethyl ether. Yield: 18 mg (71%). The obtained complex was identified as *mer-[6]PF₆* by IR spectroscopy and CV.

cis,mer-[RuCl(OH)(NO)(ebpea)]PF₆ (mer-[7]PF₆). Procedure A. K₂[RuCl₅(NO)] (100 mg, 0.26 mmol) and ebpea (66 mg 0.26 mmol) were suspended in H₂O (15 cm³). This mixture was refluxed for 30 min to give a dark brown solution. The volume of this solution was reduced, and NH₄PF₆ (120 mg) was added as a precipitant. The brown product obtained was collected by filtration and washed with H₂O, C₂H₅OH, and diethyl ether. Yield: 90 mg (58%). Anal. Calcd for C₁₆H₂₄N₄O₃-F₆PClRu: C, 31.93; H, 4.02; N, 9.31. Found: C, 32.35; H, 3.76; N, 9.39. $\nu(\text{NO})$: 1844, 1860 (KBr), 1844 cm⁻¹ (in CH₃CN). ¹H NMR indicated that the obtained complex was a mixture of isomers. MS (FAB⁺): *m/z* 439 (M – PF₆).

Procedure B. mer-[6]PF₆ (50 mg, 0.042 mmol) and KCl (30 mg, 0.40 mol) were suspended in H₂O (10 cm³). This suspension was refluxed for 3 h to give a brown solution. The volume of the solution was reduced, and NH₄PF₆ (70 mg) was added as a precipitant. The brown product obtained was collected by filtration and washed with H₂O, C₂H₅OH, and diethyl ether. Yield: 36 mg (74%). The obtained complex was identified as *mer-[7]PF₆* by IR spectroscopy and CV.

Reaction of mer-[1] or mer-[2] in H₂O–C₂H₅OH To Afford fac-[1]. mer-[1] or mer-[2] (20 mg) was suspended in H₂O–C₂H₅OH (2:3 v/v) 10 cm³. The suspension was refluxed for 2 h to give a homogeneous solution. The volume of the solution was reduced to dryness with a rotary evaporator. To the light brown residual, H₂O was added. The complex was collected by filtration and washed with H₂O, C₂H₅OH, and diethyl ether. The obtained complex was identified as *fac-[1]* by CV and UV–vis spectroscopy. Yield: 17 mg (85%) as a source of *mer-[1]*, 16 mg (80%) as a source of *mer-[2]*.

Reaction of mer-[1] in CH₃OH To Afford mer-[2]. mer-[1] (20 mg) was suspended in CH₃OH (5 cm³). The suspension was refluxed for 1 h to give a suspended orange solution. The dark brown product obtained

Table 1. Crystallographic Data of Ruthenium Complexes

	<i>fac</i> -[1]	<i>mer</i> -[2]	<i>mer</i> -[3](PF ₆) ₂
formula	C ₁₆ H ₂₁ N ₃ Cl ₃ Ru	C ₁₆ H ₂₀ N ₃ Cl ₃ Ru	C ₂₂ H ₃₀ N ₆ F ₁₂ P ₂ Ru
fw	462.79	461.78	769.52
cryst syst	monoclinic	monoclinic	triclinic
space group	P2 ₁ /n (no. 14)	P2 ₁ /c (no. 14)	P-1 (no. 2)
<i>a</i> /Å	7.7766(2)	7.5561(5)	12.5691(2)
<i>b</i> /Å	14.6864(4)	15.3044(9)	13.1846(2)
<i>c</i> /Å	15.2361(5)	15.2179(10)	18.6141(4)
α /deg			86.411(3)
β /deg	100.2047(5)	104.439(4)	83.310(3)
γ /deg			78.752(3)
<i>V</i> /Å ³	1712.59(9)	1704.24(19)	3002.33(9)
<i>Z</i>	4	4	4
<i>D</i> _{calcd} /g cm ⁻³	1.795	1.800	1.702
μ (Mo K α)/cm ⁻¹	13.847	13.913	7.285
<i>T</i> /°C	–180	–180	–180
no. of reflns	13 172	12 924	23 635
no. of unique reflns	3918	3885	13157
<i>R</i> / <i>wR</i> ^a	0.0284/0.0618	0.0500/0.0905	0.0469/0.1010
GOF	1.059	1.187	1.057

^a $R = \frac{\sum |F_o| - |F_c|}{\sum |F_o|}$ ($I > 2\sigma(I)$). $wR = \frac{[\sum (w(F_o^2 - F_c^2))^2]}{\sum (w(F_o^2))^2}^{1/2}$ (all reflections).

was collected by filtration and washed with H₂O, C₂H₅OH, and diethyl ether. The obtained complex was identified as *mer-[2]* by CV and UV–vis spectroscopy. Yield: 12 mg (60%).

Similar reactions were carried out: (1) under an argon atmosphere to give *mer-[2]* in ca. 60% yield; (2) the starting suspension in the presence of concentrated hydrochloric acid afforded a mixture of *mer-[2]* and *mer-[1]*.

Reaction of mer-[3](PF₆)₂ in H₂O–C₂H₅OH To Afford fac-[1]. mer-[3](PF₆)₂ (30 mg) was suspended in H₂O–C₂H₅OH (1:4 v/v) 10 cm³ containing hydrochloric acid (37%, 0.15 cm³). The suspension was stirred for 30 h, and the volume of the solution was reduced with a rotary evaporator to give a brown solid. The complex was collected by filtration and washed with H₂O, C₂H₅OH, and diethyl ether. The obtained complex was identified as *fac-[1]* by CV and UV–vis spectroscopy. Yield: 8 mg (44%).

A similar reaction of *mer-[3](PF₆)₂* (50 mg) was carried under refluxing conditions to give *fac-[1]*. Yield: 22 mg (73%).

Reaction of fac-[4]PF₆ with Hydrochloric Acid To Afford mer-[4]PF₆. fac-[4]PF₆ (25 mg) was suspended in H₂O (5 cm³) with hydrochloric acid (37%, 0.4 cm³). The suspension was refluxed for 1 h to give a reddish brown solution. The volume of the solution was reduced with a rotary evaporator, and NH₄PF₆ (50 mg) was added as a precipitant to give a reddish brown solid. The solid was collected by filtration and washed with H₂O, C₂H₅OH, and diethyl ether. The obtained complex was identified as *mer-[4]PF₆* by IR and UV–vis spectroscopies and CV. Yield: 20 mg (80%).

Reaction of fac-[5]PF₆ with Hydrochloric Acid To Afford fac-[4]PF₆. fac-[5]PF₆ (50 mg) was suspended in hydrochloric acid (37%, 5.0 cm³). The suspension was refluxed for 10 min to give a reddish brown solution. The volume of the solution was reduced with a rotary evaporator, and NH₄PF₆ (500 mg) was added as a precipitant to give a reddish brown solid. The solid was collected by filtration and washed with H₂O, C₂H₅OH, and diethyl ether. The obtained complex was identified as *fac-[4]PF₆* by IR and UV–vis spectroscopies and CV. Yield: 40 mg (88%).

Reaction of mer-[6]PF₆ or mer-[7]PF₆ with Hydrochloric Acid To Afford mer-[4]PF₆. The starting complex, mer-[6]PF₆ (50 mg) or *mer-[7]PF₆* (50 mg), was suspended in hydrochloric acid (37%,

Table 2. Crystallographic Data of Nitrosylruthenium Complexes

	<i>fac</i> -[4]PF ₆	<i>mer</i> -[4]PF ₆	<i>fac</i> -[5]PF ₆ ·0.5CH ₃ CN	<i>mer</i> -[6]PF ₆	<i>mer</i> -[7]PF ₆
formula	C ₁₆ H ₂₁ N ₄ O ₆ F ₆ Cl ₂ PRu	C ₁₆ H ₂₁ N ₄ O ₆ F ₆ Cl ₂ PRu	C ₁₇ H _{22.5} N _{6.5} O ₇ F ₆ PRu	C ₁₇ H ₂₄ N ₄ O ₂ F ₆ ClPRu	C ₁₆ H ₂₂ N ₄ O ₂ F ₆ ClPRu
fw	602.31	602.31	675.94	597.89	583.86
cryst syst	monoclinic	monoclinic	triclinic	monoclinic	monoclinic
space group	<i>P</i> 2 ₁ / <i>c</i> (no. 14)	<i>P</i> 2 ₁ / <i>c</i> (no. 14)	<i>P</i> -1 (no. 2)	<i>P</i> 2 ₁ / <i>n</i> (no. 14)	<i>P</i> 2 ₁ / <i>c</i> (no. 14)
<i>a</i> /Å	13.113(3)	8.3476(5)	7.90440(10)	7.5277(2)	8.7574(2)
<i>b</i> /Å	10.716(2)	30.1065(14)	10.8652(2)	17.5563(5)	12.0307(4)
<i>c</i> /Å	15.505(3)	8.8442(5)	14.2991(2)	17.0294(9)	19.8994(8)
α /deg			82.366(6)		
β /deg	101.1701(8)	110.5817(5)	77.342(6)	101.9969(7)	98.6112(5)
γ /deg			79.744(6)		
<i>V</i> /Å ³	2137.5(7)	2080.83(20)	1173.41(3)	2201.43(14)	2072.92(12)
<i>Z</i>	4	4	2	4	4
<i>D</i> _{calcd} /g cm ⁻³	1.871	1.922	1.913	1.804	1.871
μ(Mo Kα)/cm ⁻¹	11.269	11.576	8.393	9.795	10.378
<i>T</i> /°C	-180	-180	-180	-180	-180
no. of reflns	16214	20212	9145	16974	15824
no. of unique reflns	4877	4732	5112	5036	4640
<i>R</i> / <i>wR</i> ^a	0.0323/0.0745	0.0683/0.1360	0.0316/0.0773	0.0685/0.1618	0.0331/0.0745
GOF	1.046	1.231	1.076	1.105	1.147

^a $R = \sum |F_o| - |F_c| / \sum |F_o|$ ($I > 2\sigma(I)$). $wR = [\sum (w(F_o^2 - F_c^2)^2) / \sum w(F_o^2)^2]^{1/2}$ (all reflections).

Table 3. Crystallographic Data of [8] and [9]

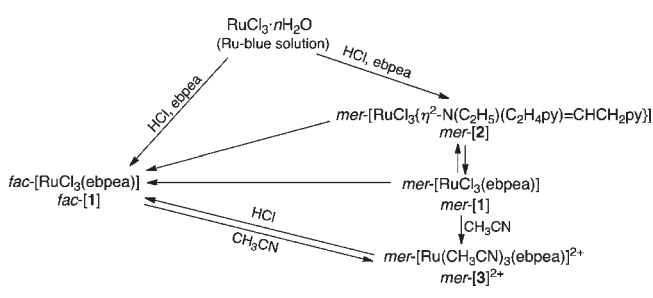
	[8]	[9]
formula	C ₁₆ H ₂₀ N ₁₀ ORu	C ₁₆ H ₂₀ N ₄ OCl ₂ Ru
fw	469.47	456.34
cryst syst	monoclinic	monoclinic
space group	<i>P</i> 2 ₁ / <i>n</i> (no. 14)	<i>P</i> 2 ₁ / <i>n</i> (no. 14)
<i>a</i> /Å	8.632(2)	8.8374(14)
<i>b</i> /Å	12.109(3)	14.573(2)
<i>c</i> /Å	17.443(5)	13.523(2)
β /deg	91.3161(11)	95.4396(5)
<i>V</i> /Å ³	1822.8(8)	1733.7(5)
<i>Z</i>	4	4
<i>D</i> _{calcd} /g cm ⁻³	1.711	1.748
μ (Mo Kα)/cm ⁻¹	8.924	12.235
<i>T</i> /°C	-180	-180
no. of reflns	13896	13220
no. of unique reflns	4173	3957
<i>R</i> / <i>wR</i> ^a	0.0249/0.0572	0.0236/0.0575
GOF	1.088	1.069

^a $R = \sum |F_o| - |F_c| / \sum |F_o|$ ($I > 2\sigma(I)$). $wR = [\sum (w(F_o^2 - F_c^2)^2) / \sum w(F_o^2)^2]^{1/2}$ (all reflections).

5.0 cm³). The suspension was refluxed for 10 min, and NH₄PF₆ was added as a precipitant to give a solid. The solid was collected by filtration and washed with H₂O, C₂H₅OH, and diethyl ether. The obtained complexes were identified as *mer*-[4]PF₆ by IR spectroscopies and CV. Yield: 50 mg (99%) for *mer*-[6]PF₆, 40 mg (77%) for *mer*-[7]PF₆.

Reactions of Nitrosylruthenium Complexes with an Azide Ion To Afford [Ru^{II}(N₃)₂{N(O)CH(py)CH₂N(C₂H₅)C₂H₄py}] ([8]). Nitrosyl complexes, *mer*-[4]PF₆ (30 mg), *fac*-[4]PF₆ (30 mg), *fac*-[5]PF₆ (33 mg), *mer*-[6]PF₆ (30 mg), and *mer*-[7]PF₆ (29 mg), were

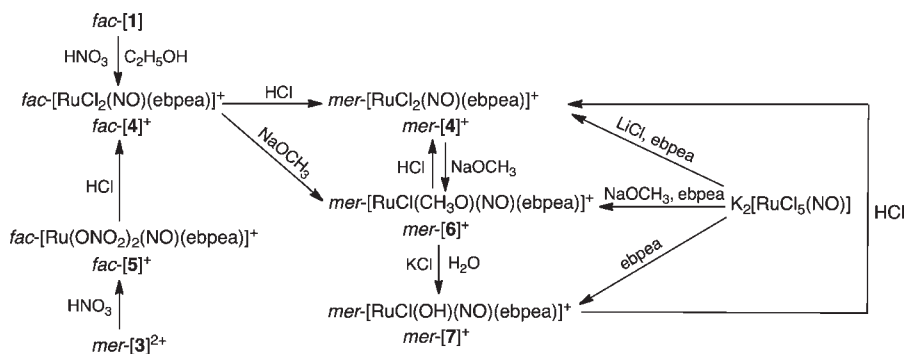
Scheme 1. Synthetic Routes of Complexes



suspended in CH₃OH (5 cm³) with NaN₃ (13 mg). The mixtures were refluxed for 5 h to give green solids. The green products obtained were collected by filtration. Yield: 68% for *fac*-[4]PF₆, 68% for *mer*-[4]PF₆, 56% for *fac*-[5]PF₆, 90% for *mer*-[6]PF₆, 86% for *mer*-[7]PF₆. Anal. Calcd for C₁₆H₂₀N₁₀ORu: C, 40.93; H, 4.29; N, 29.84. Found: C, 41.04; H, 4.40; N, 29.85. ν(NO): 1408 cm⁻¹ (KBr). ¹H NMR (CD₃NO₂, 300 MHz): δ 1.03 (3H, t, J = 7.2 Hz, CH₃(ethyl)), 1.86 (1H, m, CH₂), 2.37 (1H, m, CH₂), 2.91 (2H, m, CH₂(ethyl)), 3.12 (1H, m, CH₂), 3.26 (1H, m, CH₂), 3.67 (1H, m, CH₂), 3.92 (1H, m, CH₂), 6.15 (1H, d, J = 4.3 Hz, CH), 7.33 (1H, d, J = 7.7 Hz, 3-H(py)), 7.46 (1H, m, 5-H(py)), 7.62 (1H, ddd, J = 1.4, 5.8, 7.7 Hz, 5-H(py)), 7.69 (1H, d, J = 7.7 Hz, 3-H(py)), 7.82 (1H, td, J = 1.4, 7.7 Hz, 4-H(py)), 8.10 (1H, td, J = 1.4, 7.7 Hz, 4-H(py)), 8.51 (1H, d, J = 5.8 Hz, 6-H(py)), 9.41 (1H, d, J = 5.8 Hz, 6-H(py)). ¹³C NMR (CD₃NO₂, 75.6 MHz): δ 8.43, 35.35, 43.77, 57.71, 59.07, 106.75, 121.49, 123.79, 126.08, 126.20, 139.66, 141.29, 153.09, 155.94, 156.85, 162.14. MS (FAB⁺): *m/z* 428 (M - N₃).

Reaction of [8] with Hydrochloric Acid To Afford [Ru^{II}Cl₂{N(O)CH(py)CH₂N(C₂H₅)C₂H₄py}] ([9]). [8] (100 mg) was suspended in CH₃OH (15 cm³) with hydrochloric acid (37%, 0.7 cm³). The suspension was refluxed for 2 h, and then the volume of the solution was reduced to dryness with a rotary evaporator. H₂O was added to the formed green solid. The complex was collected by filtration and washed with H₂O, CH₃OH,

Scheme 2. Synthetic Routes of Nitrosyl Complexes



and diethyl ether. Yield: 81 mg (85%). Anal. Calcd for $C_{16}H_{20}N_4Cl_2Ru$: C, 42.11; H, 4.42; N, 12.28. Found: C, 41.73; H, 4.46; N, 12.33. $\nu(\text{NO})$: 1415 cm^{-1} (KBr). $^1\text{H NMR}$ (CD_3NO_2 , 300 MHz): δ 1.00 (3H, t, $J = 7.2$ Hz, CH_3 (ethyl)), 1.76 (1H, m, CH_2), 2.39 (1H, m, CH_2), 2.89 (2H, m, CH_2 (ethyl)), 3.02 (1H, m, CH_2), 3.66 (2H, m, CH_2), 3.92 (1H, d, $J = 13.9$ Hz, CH_2), 6.23 (1H, d, $J = 4.5$ Hz, CH), 7.27 (1H, d, $J = 7.2$ Hz, 3-H(py)), 7.34 (1H, ddd, $J = 1.4, 5.8, 7.7$ Hz, 5-H(py)), 7.53 (1H, ddd, $J = 1.4, 5.8, 7.7$ Hz, 5-H(py)), 7.63 (1H, d, $J = 7.7$ Hz, 3-H(py)), 7.77 (1H, td, $J = 1.4, 7.7$ Hz, 4-H(py)), 8.06 (1H, td, $J = 1.4, 7.7$ Hz, 4-H(py)), 8.63 (1H, d, $J = 5.8$ Hz, 6-H(py)), 9.96 (1H, d, $J = 5.8$ Hz, 6-H(py)). $^{13}\text{C NMR}$ (CD_3NO_2 , 75.6 MHz): δ 8.51, 30.78, 35.38, 57.88, 59.22, 107.64, 109.84, 121.04, 122.90, 125.35, 125.61, 139.36, 141.09, 154.58, 158.59.

X-ray Crystallography. Single crystals of *fac*-[1] and *mer*-[6]PF₆ were obtained by slow evaporation of their reaction solutions and those of *mer*-[2] from its CH_3NO_2 solution. Those of *mer*-[3](PF₆)₂ and *mer*-[4]PF₆ were obtained by recrystallization from a CH_3CN solution, *fac*-[4]PF₆, *fac*-[5]PF₆·0.5 CH_3CN , and *mer*-[7]PF₆ were obtained by recrystallization from a CH_3CN solution containing a small amount of water, and [8] and [9] were obtained by recrystallization from a CH_3NO_2 solution and then vapor diffusion of ether into the solution. The crystallographic data are summarized in Tables 1–3. Intensity data were collected on a Rigaku Mercury CCD diffractometer using graphite-monochromated Mo K α radiation (0.71069 Å). All calculations were carried out using the Crystal Structure software package.⁹ Structures were solved by direct methods, expanded using Fourier techniques, and refined using full-matrix least-squares techniques on F^2 using SHELXL97.¹⁰

Computational Details. DFT calculations of *mer*-[2] were performed at the B3LYP¹¹/LANL2DZ¹² level, which consists of a hybrid Becke + Hartree–Fock exchange and Lee–Yang–Parr correlation functional with nonlocal corrections, with the LANL2DZ effective core potential and basis set using the Gaussian 03 program.¹³ Starting from the crystal structure, the geometry optimizations were carried out under the diamagnetic and paramagnetic conditions without any symmetric constraint.

RESULTS AND DISCUSSIONS

Syntheses of Trichloro and Triacetonitrile Complexes. Syntheses and reactions of Ru(III) and Ru(II) complexes are summarized in Scheme 1, and all synthetic procedures were carried out under an air atmosphere. Two trichlororuthenium(III) complexes bearing ebpea, *fac*- and *mer*-[Ru^{III}Cl₃(ebpea)] (*fac*- and *mer*-[1]), and one trichloro complex bearing $\eta^2\text{-N}(\text{C}_2\text{H}_5)(\text{C}_2\text{H}_4\text{py})=\text{CHCH}_2\text{py}$, which was formed by C–H activation of an alkyl chain between the amine nitrogen atom and the pyridyl ring, *mer*-[Ru^{III}Cl₃{ $\eta^2\text{-N}(\text{C}_2\text{H}_5)(\text{C}_2\text{H}_4\text{py})=\text{CHCH}_2\text{py}$ }] (*mer*-[2]), were synthesized. Syntheses of *fac*-[1] and *mer*-[2] were carried out under several reaction conditions using the Ru–blue solution with hydrochloric

acid, sulfuric acid, or potassium chloride. In the presence of hydrochloric acid, a yield of *mer*-[2] was increased with increasing concentration of hydrochloric acid to 42%, while that of *fac*-[1] was decreased with increasing concentration of hydrochloric acid. Reactions using sulfuric acid or potassium chloride afforded mixtures of *fac*-[1], *mer*-[2], and unidentified complexes without formation of *mer*-[Ru^{III}Cl₃(ebpea)], *mer*-[1]. These results indicated that both acid and chloride ion were necessary for the formation of *mer*-[2]. It is known that reaction products from the Ru–blue cluster are dependent upon reaction conditions.¹⁴ In our previous report, *mer*-[2] oxidized alcohols such as ethanol and 2-propanol to acetaldehyde and acetone with formation of *mer*-[1].⁶ It is likely that complex *mer*-[2] was formed via C–H activation of the (Ru–amine) moiety of *mer*-[1].

Trichlororuthenium(III) complexes, *fac*- and *mer*-[1], were used as precursors for syntheses of new ruthenium complexes. Reactions of *fac*- and *mer*-[1] in H_2O – $\text{C}_2\text{H}_5\text{OH}$ – CH_3CN under refluxing conditions for 5 h afforded a triacetonitrile ruthenium(II) complex, *mer*-[Ru^{II}(CH₃CN)₃(ebpea)]²⁺ (*mer*-[3]²⁺), in good yield. Similar reactions of chlororuthenium(III) complexes with reductant such as ethanol, Zn, and $\text{N}(\text{C}_2\text{H}_5)_3$ have been reported.^{4a,d,5} The Ru(III) species were reduced to the Ru(II) one with dissociation of the chloro ligands and association of new coming ligands.

Syntheses of Nitrosylruthenium Complexes. Syntheses and reactions of {RuNO}⁶-type nitrosyl complexes are summarized in Scheme 2.

Nitrosylruthenium complexes are synthesized using NO gas, nitrite ion, or nitrate ion as a source of a nitrosyl ligand.¹⁵ *fac*-[RuCl₂(NO)(ebpea)]PF₆, *fac*-[4]PF₆, and *fac*-[Ru(ONO₂)₂(NO)(ebpea)]PF₆, *fac*-[5]PF₆, were obtained by nitrosylation reactions of *fac*-[1] and *mer*-[3](PF₆)₂ with an ethanoic or aqueous HNO₃ solution in 83% and 41% yields. Since *fac*-[5]PF₆ was highly soluble toward organic solvents as compared to other nitrosylruthenium complexes, isolation of *fac*-[5]PF₆ was difficult from organic solvent. Synthesis of *fac*-[5]PF₆ was carried out in H_2O , and a yield of *fac*-[5]PF₆ was lower than that of *fac*-[4]PF₆. In the nitrosylation reaction by nitrate, an electron source is necessary for formation of a nitrosyl ligand. Reactions of $\text{K}_2[\text{RuCl}_5(\text{NO})]$ with an equimolar amount of ebpea afforded *mer*-[RuClX(NO)(ebpea)]PF₆ (X = Cl; *mer*-[4]PF₆, X = CH₃O; *mer*-[6]PF₆, and X = OH; *mer*-[7]PF₆), dependent on solvent and coexisting species in a reaction mixture. Reactions of *fac*- and *mer*-[4]PF₆ with NaOCH₃ in CH_3OH gave *mer*-[6]PF₆ in analogy with formation of *mer*-[RuCl(CH₃O)(NO)(ebpma)]⁺ by reaction of [RuCl₂(NO)(ebpma)]⁺.⁵ An aqueous solution of *mer*-[6]PF₆ in the presence of excess KCl gave

Table 4. Selected Bond Distances (Angstroms) and Angles (degrees) for Ruthenium Complexes

	<i>fac</i> -[1]	<i>mer</i> -[2]	<i>mer</i> -[3](PF ₆) ₂
Ru–N(amine)	2.2013(18)	2.154(3)	2.146(2)
Ru–N(py)	2.0961(17)	2.083(3)	2.109(2)
	2.1255(16)	2.113(3)	2.097(2)
Ru–X (<i>trans</i> -amine) ^a	X = Cl	X = Cl	X = CH ₃ CN
	2.3703(6)	2.3853(10)	2.037(2)
Ru–X (<i>cis</i> -amine) ^b	X = Cl	X = Cl	X = CH ₃ CN
	2.3507(4)	2.3822(10)	2.018(2)
	X = Cl	X = Cl	X = CH ₃ CN
	2.3852(4)	2.4333(11)	2.030(2)
		Y = C	
		2.101(4)	
X–Ru–Y	88.61(2)	84.66(3)	87.61(9)
	84.772(18)	80.75(3)	86.10(9)
	90.012(16)	169.98(10)	173.71(9)
N(py)–Ru–N(amine)	88.21(7)	90.99(12)	89.35(8)
	93.46(6)	90.90(11)	92.51(8)
N(py)–Ru–N(py)	93.37(6)	176.89(15)	177.97(8)
N(amine)–Ru–X(<i>trans</i> -amine)	174.56(4)	169.98(10)	178.88(9)
C(ethyl)–N(amine)–C(ethylene)	109.68(15)	121.4(3)	110.5(2)
	108.35(16)	111.3(2)	107.5(2)
C(ethylene)–N(amine)–C(ethylene)	106.12(15)	117.4(3)	107.3(2)

^aThe ligand located at the trans position toward the amine nitrogen atom. ^bLigands located at the cis position toward the amine nitrogen atom.

Table 5. Selected Bond Distances (Angstroms) and Angles (degrees) for Nitrosylruthenium Complexes

	<i>fac</i> -[4]PF ₆	<i>mer</i> -[4]PF ₆	<i>fac</i> -[5]PF ₆ ·0.5CH ₃ CN	<i>mer</i> -[6]PF ₆	<i>mer</i> -[7]PF ₆
Ru–N(amine)	2.1982(19)	2.174(3)	2.147(2)	2.172(3)	2.1555(19)
Ru–N(py)	2.112(2)	2.147(4)	2.1217(19)	2.113(3)	2.1271(18)
	2.1293(17)	2.106(4)	2.1208(18)	2.124(4)	2.1032(18)
Ru–X (<i>trans</i> -amine) ^a	X = Cl	X = Cl	X = ONO ₂	X = Cl	X = Cl
	2.3857(5)	2.4136(12)	2.1219(19)	2.3828(14)	2.4011(6)
Ru–Y (<i>cis</i> -amine)	Y = Cl ^c	Y = Cl ^b	Y = ONO ₂ ^c	Y = OCH ₃ ^b	Y = OH ^b
	2.3711(6)	2.3259(10)	2.0631(15)	1.954(4)	1.9375(17)
Ru–N(NO)	1.7467(18)	1.771(3)	1.7603(18)	1.816(3)	1.763(2)
N–O(NO)	1.142(2)	1.135(5)	1.133(2)	1.107(5)	1.141(3)
X–Ru–Y	89.389(9)	87.03(4)	83.13(7)	86.25(13)	84.85(5)
X–Ru–N(NO)	85.90(6)	84.32(13)	94.90(8)	87.83(13)	91.01(7)
Y–Ru–N(NO)	88.31(6)	169.49(16)	99.45(7)	173.98(18)	175.64(8)
N(py)–Ru–N(amine)	89.37(7)	94.22(16)	91.18(8)	93.44(13)	89.50(7)
	93.85(7)	85.48(16)	94.54(7)	88.43(16)	92.42(7)
N(py)–Ru–N(py)	87.31(7)	172.07(12)	88.53(7)	176.16(16)	177.93(7)
N(amine)–Ru–X(<i>trans</i> -amine)	176.24(5)	173.85(12)	171.89(7)	175.09(10)	172.81(5)
Ru–N–O(NO)	167.9(2)	169.3(4)	177.17(17)	169.3(4)	170.01(19)
C(ethyl)–N(amine)–C(ethylene)	107.09(16)	111.0(3)	108.9(2)	107.8(3)	110.97(17)
	109.06(17)	107.6(3)	107.99(16)	111.7(3)	108.19(17)
C(ethylene)–N(amine)–C(ethylene)	108.95(18)	107.4(3)	108.3(2)	107.7(3)	108.27(18)

^aThe ligand located at the trans position toward the amine nitrogen atom. ^bLigands located at the cis position toward the amine nitrogen atom. Ligands located at the trans position toward the NO ligand. ^cLigands located at the cis position toward the NO ligand.

mer-[7]PF₆, which was formed via substitution of the methoxy ligand by a hydroxo ligand. *mer*-[4]⁺ was formed by reactions of *fac*-[4]PF₆, *mer*-[6]PF₆, and *mer*-[7]PF₆ in hydrochloric acid solutions. It is noteworthy that *fac*-[4]⁺ changes into *mer*-[4]⁺, indicating that the meridional form is more stable than the facial form under

these conditions and stabilities of the ebpea complexes differ from those of the ebpma complexes.

Structures of Complexes. Selected bond distances and angles of *mer*-[3](PF₆)₂ are summarized in Table 4 with those of reported complexes, *fac*-[1] and *mer*-[2],⁶ and those of nitrosyl

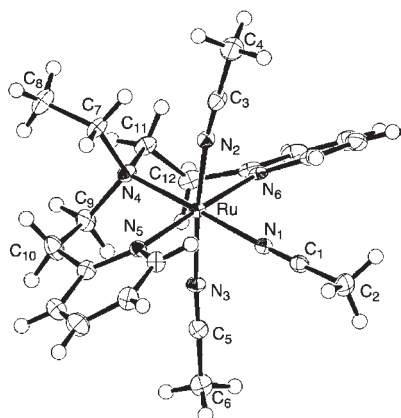


Figure 2. Structure of $mer\text{-}[\text{Ru}(\text{CH}_3\text{CN})_3(\text{ebpea})]^{2+}$ ($mer\text{-}[3]^{2+}$).

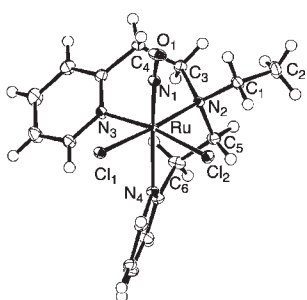


Figure 3. Structure of $fac\text{-}[\text{RuCl}_2(\text{NO})(\text{ebpea})]^+$ ($fac\text{-}[4]^+$).

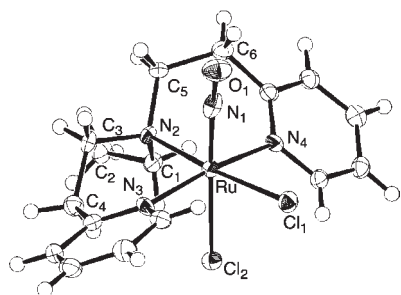


Figure 4. Structure of $mer\text{-}[\text{RuCl}_2(\text{NO})(\text{ebpea})]^+$ ($mer\text{-}[4]^+$).

complexes, $fac\text{-}[4]\text{PF}_6$, $mer\text{-}[4]\text{PF}_6$, $fac\text{-}[5]\text{PF}_6 \cdot 0.5\text{CH}_3\text{CN}$, $mer\text{-}[6]\text{PF}_6$, and $mer\text{-}[7]\text{PF}_6$, in Table 5. Structures of these complexes are shown in Figures 2–7, indicating octahedral geometry around the Ru center. Structures of all complexes, $[\text{RuXYZ}(\text{ebpea})]^n$, revealed that three nitrogen atoms of the ebpea and three coexisting ligands were located in octahedral ideal positions around the ruthenium center by comparison corresponding to ebpa complexes.⁵ The bond angles between the ancillary ligands such as Cl, CH_3CN , NO, CH_3O , OH, and ONO_2 and the ruthenium center ($\text{X}-\text{Ru}-\text{X}$, $\text{X}-\text{Ru}-\text{Y}$, $\text{X}-\text{Ru}-\text{N}(\text{nitrosyl})$, and $\text{Y}-\text{Ru}-\text{N}(\text{nitrosyl})$) were also close to the ideal right angle or straight angle. The ebpea ligand coordinated in both the *fac* and the *mer* fashion with one amine and two pyridyl nitrogen atoms. Structures of three facial-type complexes and five meridional-type complexes were determined. In nitrosyl complexes, electron-donor ligands such CH_3O^- and OH^- of $mer\text{-}[6]\text{PF}_6$ and $mer\text{-}[7]\text{PF}_6$ were favorably located in the trans position toward the nitrosyl ligand owing to its strong electron-donor character. The nitrate ligand, ONO_2^- ,

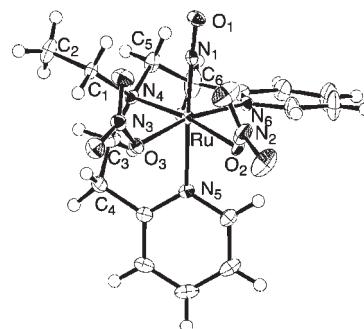


Figure 5. Structure of $fac\text{-}[\text{Ru}(\text{ONO}_2)_2(\text{NO})(\text{ebpea})]^+$ ($fac\text{-}[5]^+$).

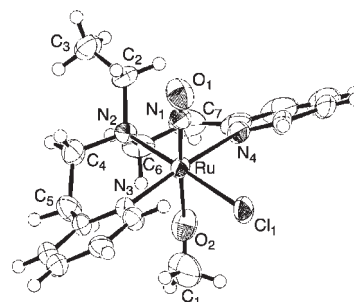


Figure 6. Structure of $mer\text{-}[\text{RuCl}(\text{CH}_3\text{O})(\text{NO})(\text{ebpea})]^+$ ($mer\text{-}[6]^+$).

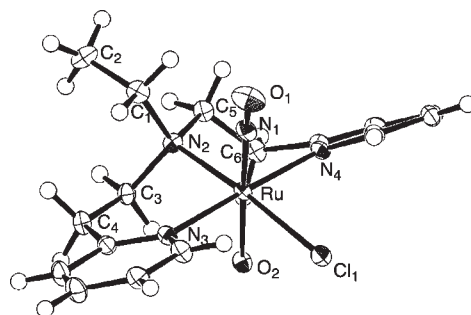


Figure 7. Structure of $mer\text{-}[\text{RuCl}(\text{OH})(\text{NO})(\text{ebpea})]^+$ ($mer\text{-}[7]^+$).

coordinated to the Ru center at the cis position toward the nitrosyl ligand and the chloro ligand at both cis and trans positions. These results indicated that the interaction between the nitrosyl and the coexisting ligands were important for regulating the coordinating geometry around the Ru center and the meridional form complexes bearing the ebpea ligand was more stabilized than that of ebpa complexes.

The bond distances between the ruthenium center and the amine nitrogen atom of the ebpea ligand, $\text{Ru}-\text{N}(\text{amine})$ (2.146–2.201 Å), were longer than those of the pyridyl nitrogen atoms, $\text{Ru}-\text{N}(\text{py})$ (2.083–2.129 Å), due to π -back-donation from the ruthenium center to the pyridine rings. The $\text{Ru}-\text{N}$ bond distances of $\text{Ru}-\text{N}(\text{amine})$ (2.146–2.201 Å) and $\text{Ru}-\text{N}(\text{py})$ (2.083–2.129 Å) of the ebpea complexes were longer than those of the ebpa complexes ($\text{Ru}-\text{N}(\text{amine}) = 2.090\text{--}2.137$ Å and $\text{Ru}-\text{N}(\text{py}) = 2.039\text{--}2.103$ Å), indicating that the ebpea ligand weakly coordinated toward the ruthenium center, compared with the ebpa complexes.⁵ The structural parameters of the $\text{Ru}-\text{NO}$ moieties, $\text{Ru}-\text{N}(\text{nitrosyl})$ (1.761–1.816 Å) and $\text{N}-\text{O}$ (1.107–1.142 Å), and the angles, $\text{Ru}-\text{N}-\text{O}$

(167.9–177.2°), were similar to those of reported {RuNO}⁶⁻-type nitrosylruthenium complexes containing the ebpma ligand.⁵ Thus, these nitrosyl complexes can be classified as a {RuNO}⁶⁻ type.^{15c} The Ru–N distances between the Ru center and the pyridyl nitrogen atoms (2.103–2.147 Å) in the nitrosyl complexes were relatively longer than those in the non-nitrosylruthenium complexes, *fac*-[1] and *mer*-[3](PF₆)₂. This lengthening tendency of the nitrosyl complexes was attributed to coordination of the strong π-acceptor nitrosyl ligand. The trans influence of the nitrosyl ligand in *mer*-[4]⁺ was observed at a shorter distance (2.3259 Å) between the ruthenium center and the chloro ligand, which was located in the trans position toward the nitrosyl ligand, than Ru–Cl distances (2.3711–2.4136 Å), which were located in the cis position toward the nitrosyl ligand. The dihedral angle between the pyridyl rings of *mer*-[4]⁺ (65°) was larger than those of the ebpma complexes (2–5°). These results suggested that two π-acceptor pyridyl rings interacted with different dπ(Ru) orbitals, and the meridional form of the ebpea complexes was stabilized compared to the ebpma complexes.

Properties of Trichloro and Triacetonitrile Complexes.

Electrochemical, infrared, and electronic spectral properties are summarized in Table 6. Cyclic voltammograms (CVs) of ruthenium(III) and (II) complexes *fac*-[1], *mer*-[1], and *mer*-[2] in CH₂Cl₂ and *mer*-[3]²⁺ in CH₃CN at –40 °C are shown in Figure 8. Solubilities of ruthenium complexes are different from each other. *mer*-[2] is less soluble in aqueous and organic solvents. CVs of both the *fac*-[1] and the *mer*-[1], Figure 8a and 8b, revealed a reversible oxidation wave and an irreversible reduction wave at 1.06 and –0.57 V for *fac*-[1] and 0.99 and –0.76 V for *mer*-[1], respectively. Reversible oxidation waves at 1.06 and 0.99 V were assigned to one-electron redox couples between Ru(III) and Ru(IV) and irreversible reduction waves at –0.57 and –0.76 V to one-electron reduction from Ru(III) to Ru(II). On the reverse scan after appearing in the reduction wave, new oxidation waves were observed at –0.06 and –0.13 V accompanying one-electron reduction. These results indicated that the reductive forms of *fac*-[1] and *mer*-[1], [Ru^{II}Cl₃(ebpea)][–], were unstable even at –40 °C and changed to unidentified species that were oxidized at around –0.1 V. The reversibility of the oxidation wave for *fac*-[1] at 25 °C was different from that at –40 °C, while the CV profiles of *mer*-[1] at 25 and –40 °C were the same, indicating the oxidation species of *fac*-[1] was unstable compared with that of *mer*-[1]. The CV of *mer*-[2] showed a reversible oxidation wave at 0.93 V assigned to oxidation of the Ru center and an irreversible reduction wave

at –1.78 V to reduction of the iminium ligand (Figure 8c). Complex *mer*-[3](PF₆)₂ showed a typical CV profile of the Ru(II) complex having one reversible redox couple at 1.10 V attributed to the Ru(III)/Ru(II) couple (Figure 8d).

The ¹H NMR signals of *mer*-[2] in (CD₃)₂SO and *mer*-[3]²⁺ in CD₃CN were observed in the normal region, indicating their diamagnetic properties.⁶ For *mer*-[2], the proton signal of the –N=CH– moiety was observed at 6.56 ppm as a doublet and those of the –N=CH–CH₂– moiety at lower magnetic region, 4.30 and 4.78 ppm. This result in addition to the structural and electrochemical results indicated the iminium ion coordination mode of the N–C moiety of *mer*-[2] was reasonable (see the latter section). For *mer*-[3]²⁺, signals of two pyridine rings and two acetonitrile, which were located in the trans position to each other, were equivalently observed.

The electronic spectra of *fac*-[1], *mer*-[1], *mer*-[2], and *mer*-[3](PF₆)₂ complexes revealed dπ(Ru)–π*(ebpea) transitions in the higher wavelength region and a π–π* transition based on ebpea in the lower wavelength region (Figure S11, Supporting Information).

Properties of Nitrosylruthenium Complexes. Five nitrosylruthenium complexes, two facial-form and three meridional-form complexes, were characterized as a {RuNO}⁶⁻-type complex from X-ray structural analyses, IR spectral data, and electrochemical properties in Table 6. CVs of nitrosylruthenium complexes,

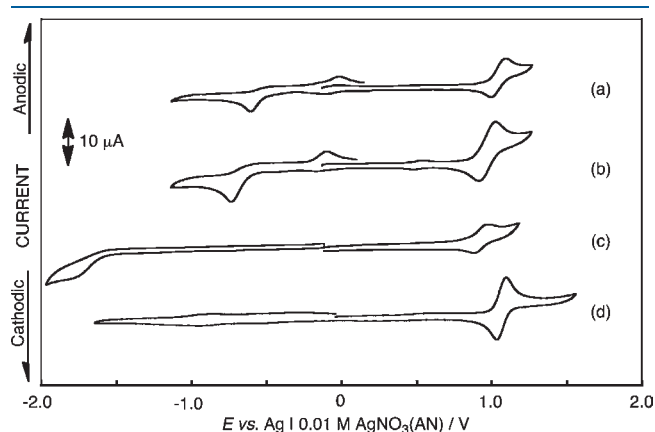


Figure 8. Cyclic voltammograms at –40 °C: (a) *fac*-[1]PF₆ (0.7 mM in CH₂Cl₂), (b) *mer*-[1]PF₆ (1.0 mM in CH₂Cl₂), (c) *mer*-[2]PF₆ (0.3 mM in CH₂Cl₂), and (d) *mer*-[3](PF₆)₂ (1.0 mM in CH₃CN).

Table 6. Redox Potentials, Characteristic NO Stretching Frequency, and Electronic Absorption Bands

complex	E/V		ν(NO)/cm ^{–1}		
	oxidation	reduction	KBr	CH ₃ CN	λ _{max} /nm (10 ^{–4} ε/M ^{–1} cm ^{–1})
<i>fac</i> -[1]	1.06	–0.57			249(0.79), 312(0.34), 356(0.28), 439(0.10)
<i>mer</i> -[1]	0.99	–0.76			241(0.97), 313(0.43), 397(0.23), 455(0.08)
<i>mer</i> -[2]	0.93	–1.78			242(1.00), 273(0.49), 300(0.51), 324(0.42)
<i>mer</i> -[3](PF ₆) ₂	1.10				242(1.18), 2.78(0.40), 321(0.93)
<i>fac</i> -[4]PF ₆		–0.46	1901	1904	263(0.71)
<i>mer</i> -[4]PF ₆		–0.48	1868	1882	256(1.02)
<i>fac</i> -[5]PF ₆		–0.25	1931	1931	
<i>mer</i> -[6]PF ₆		–0.99	1817	1833	265(1.11), 390(0.05)
<i>mer</i> -[7]PF ₆		–1.00	1844, 1860	1844	258(0.92)
[8]	0.56	–1.71	1408		247(1.55), 375(0.82)
[9]	0.71	–1.73	1415		245(0.86), 362(0.77)

fac-[4]PF₆, *mer*-[4]PF₆, *fac*-[5]PF₆, *mer*-[6]PF₆, and *mer*-[7]PF₆, in CH₃CN showed a one-electron reduction wave assigned to reduction of the (RuNO)³⁺ moiety in a similar manner to {RuNO}⁶-type complexes.^{5,16} The CV profiles of *fac*- and *mer*-[RuCl₂(NO)(ebpea)]⁺ ([4]⁺) were similar to each other and showed a reversible redox couple at -0.46 V for the *fac*-form complex and -0.48 V for the *mer*-form one. CVs of *fac*-[5]⁺, *mer*-[6]⁺, and *mer*-[7]⁺ showed an irreversible reduction wave at -0.25, -0.99, and -1.00 V based on (RuNO)^{3+/2+} reduction, respectively. The reduction potential values of these nitrosylruthenium complexes were dependent on the nature of the ancillary ligands such as Cl⁻, ONO₂⁻, CH₃O⁻, and OH⁻. The reduction potentials were correlated with the values of the stretching N–O mode ($\nu(\text{NO})$) in IR spectroscopy and the structural parameters of the (RuNO) moieties. Nitrosylruthenium complexes showed a strong NO stretching vibration at 1817–1931 (in KBr disk) and 1833–1931 cm⁻¹ (in CH₃CN solution) (Table 6). These observed values of the $\nu(\text{NO})$ band were similar to those of {RuNO}⁶-type nitrosylruthenium complexes previously reported.^{5,16} The electronic spectra of *fac*-[4]PF₆, *mer*-[4]PF₆, *fac*-[5]PF₆, *mer*-[6]PF₆, and *mer*-[7]PF₆ are shown in Figure S12, Supporting Information, and maximum absorption wavelengths with ϵ are summarized in Table 6. The electronic spectra of nitrosylruthenium complexes revealed a $d\pi(\text{Ru})-\pi^*(\text{ebpea})$ transition in the lower wavelength region (Figure S12, Supporting Information), owing to stabilization of $d\pi(\text{Ru})$ orbitals by the strong π -acid NO ligand. The structural parameters of the (RuNO) moieties, the Ru–N and N–O distances, and the Ru–N–O angle also were related to properties of nitrosylruthenium complexes, and these values were equivalent to those of {RuNO}⁶-type nitrosylruthenium complexes containing polypyridine ligand such as bpy, trpy,¹⁷ and ebpma.⁵ Reduction potential and $\nu(\text{NO})$ values are in a linear relationship as shown in Figure S18, Supporting Information. The coordination mode of the ebpea ligand in the series of [RuXY(NO)(ebpea)]⁺ complexes seems to be affected by the electron density of the ruthenium center, which is inferred by the reduction potentials and $\nu(\text{NO})$ values. As summarized in Figure S18, Supporting Information, electron-deficient complexes with higher potentials and $\nu(\text{NO})$ values have a facial ebpea ligand, whereas electron-rich complexes with lower values have a meridional one. The values of the dichloro complexes [RuCl₂(NO)(ebpea)]⁺ ([4]⁺), for which both facial and meridional isomers could be isolated, proved to lie in the middle. The ¹H NMR spectra of the nitrosyl complexes in CD₃CN are shown in Figure S15, Supporting Information. The spectral patterns of *mer*- and *fac*-forms were different. The *mer*-form complexes showed nine signals for the ebpea ligand consisting of two signals for the ethyl group bonded to the amine nitrogen (CH₃CH₂ and CH₃CH₂), four signals for the pyridyl groups, and three signals for the bridging groups. The *fac*-type complexes showed more complicated signal patterns than those of the *mer*-type complexes.

Conversion Between *fac*- and *mer*-Form Complexes. Reactions of trichloro and triacetonitrile complexes are summarized in Scheme 1. Conversion from *mer*-[1] to *fac*-[1] occurred in a H₂O–C₂H₅OH solution under refluxing conditions in a 85% yield, and *fac*-[1] was also obtained from *mer*-[2] under similar conditions in good yield. Hydrogen transfer to *mer*-[2] and subsequent isomerization from a meridional form to a facial form afforded *fac*-[1], indicating the trichloro complex having the ebpea ligand preferred a facial fashion. The similar isomerization reaction of the *mer* type to the *fac* type was reported in the trichlororuthenium(III) complex containing the ebpma ligand.⁵

Conversion from a facial form bearing ebpea to a meridional form occurred in a reduction of trichlororuthenium(III), *fac*-[1], in the presence of acetonitrile to give triacetonitrileruthenium(II), *mer*-[3]²⁺, although a corresponding triacetonitrile complex bearing ebpma was in a facial configuration. The configurational change from a *mer* form to a *fac* form was observed in a reaction of *mer*-[3]²⁺ with HCl to afford *fac*-[1]. In the case of ebpma complexes, the changes from the facial to the meridional configuration occurred only in nitrosyl complexes due to strong interaction between the nitrosyl ligand and π -donor coexisting ligand that coordinated at the trans position toward the nitrosyl. These results will be explained by interactions between coexisting ligands and two pyridyl groups of ebpea, being more flexible than ebpma.

Formation of *fac*-[5]PF₆ from *mer*-[3](PF₆)₂ was accompanied with a configuration change owing to interactions between the nitrosyl ligand and the ebpea and ancillary ligands. The ONO₂⁻ ligands of *fac*-[5]PF₆ have more electron-withdrawing character than a pyridyl group of ebpea. The ONO₂⁻ ligands are preferred in the cis position toward the nitrosyl ligand rather than the pyridine ring. The methoxy ligand of *mer*-[6]PF₆, the hydroxo ligand of *mer*-[7]PF₆, and the nitrate ligand of *fac*-[5]PF₆ were easily substituted by chloride ions in the presence of concentrated hydrochloric acid to give a corresponding chloro complex, [RuCl₂(NO)(ebpea)]⁺ ([4]⁺). Conversion from *fac*-[4]⁺ to *mer*-[4]⁺ occurred in dilute hydrochloric acid solution. These results indicated that the difference in stability between the facial and the meridional form was decreased due to flexible alkyl arms of ebpea as compared to ebpma. While facial forms were more stable than meridional forms of ebpma complexes,⁵ meridional forms of ebpea complexes were stabilized due to the flexibility of the ebpea ligand and interaction between the pyridyl groups and the $d\pi(\text{Ru})$ orbitals.

Two Different Types of C–H Bond Cleavage at the Ethylene Arm. Formation of *mer*-[2] in the reaction using the Ru–blue solution proceeded via oxidation of an amine group of ebpea, and *mer*-[2] changed into *mer*-[1] with accompanying oxidation of alcohol (see Supporting Information, Scheme S3). Reaction of *mer*-[2] with CD₃OD was carried out to afford a trichlororuthenium(III) complex, which showed paramagnetic property, and the formed paramagnetic trichloro complex was reduced in H₂O–C₂H₅OH–CH₃CN to give a deuterated complex, *mer*-[Ru^{II}(CH₃CN)₃{N(C₂H₅)(C₂H₄py)-CDHCH₂py}]²⁺, which was confirmed by ¹H NMR spectroscopy. Complex *mer*-[2] was regenerated by refluxing *mer*-[1] in methanol under air or argon, while reaction of *fac*-[1] under the same reaction conditions did not produce *mer*-[2]. Formation of the iminium moiety from *mer*-[1] would proceed via interaction between the ruthenium center and the C–H bond of the arm and does not require any oxidants. In the reaction of *mer*-[1] in *i*-C₃H₇OH at ca. 80 °C, dihydrogen from the gas phase and acetone from the liquid phase were confirmed by gas chromatography, and a mixture of *mer*-[1] and *mer*-[2] was obtained from the resulting suspension solution, indicating that the conversion reactions between *mer*-[1] and *mer*-[2] were not simple redox reaction. Although these reactions were very slow at room temperature and *mer*-[2] was less soluble in alcohols, 1.5 mol equiv of acetaldehyde was detected in the reaction of *mer*-[2] with C₂H₅OH and 1.2 mol equiv of acetone was detected in the reaction with *i*-C₃H₇OH. These reactions might be useful as a catalytic oxidation of alcohols. The –N(Et)–CH– moiety of *mer*-[2] can be described as structures in Chart 1, and the formal oxidation states are assigned. To gain more insight into *mer*-[2], DFT calculations have been

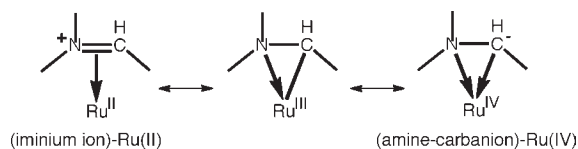
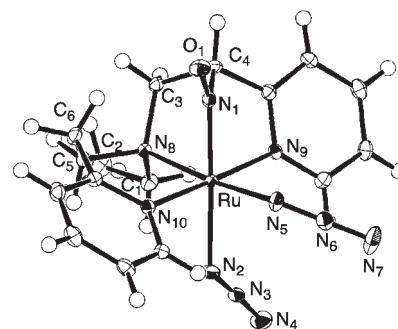
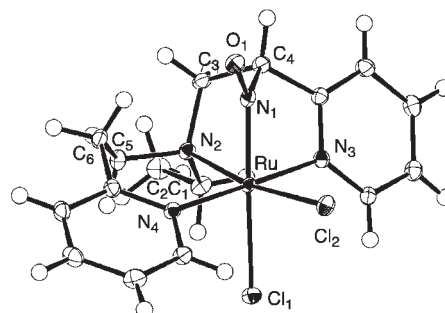
Chart 1. Possible Structures for *mer*-[2]

Table 7. Selected Bond Distances (Angstroms) and Angles (degrees) for [8] and [9]

	[8]	[9]
Ru–N(amine)	2.1867(14)	2.2106(14)
Ru–N(py)	2.0728(14)	2.0456(13)
	2.0954(15)	2.1179(13)
Ru–X		
<i>trans</i> -amine ^a	X = N ₃	X = Cl
	2.0940(15)	2.3901(4)
Ru–Y		
<i>cis</i> -amine ^b	Y = N ₃	Y = Cl
	2.1227(15)	2.4410(4)
Ru–N(NO)	1.8689(14)	1.8599(14)
N–O(NO)	1.2504(19)	1.244(2)
N(NO)–C	1.514(2)	1.516(2)
X–Ru–Y	89.57(6)	91.192(15)
X–Ru–N(NO)	94.60(6)	92.70(4)
Y–Ru–N(NO)	175.61(6)	173.52(4)
N(amine)–Ru–N(NO)	79.67(5)	79.98(6)
N(py)–Ru–N(NO)	81.01(5)	82.03(6)
	96.14(6)	97.63(5)
N(py)–Ru–N(amine)	86.61(5)	84.04(5)
	94.52(5)	95.42(5)
N(py)–Ru–N(py)	176.71(5)	179.40(5)
N(amine)–Ru–X(<i>trans</i> -amine)	174.25(5)	170.27(3)
Ru–N–O(NO)	136.71(12)	135.98(11)
C(ethyl)–N(amine)–C(ethylene)	109.93(13)	110.07(13)
	109.00(12)	108.67(13)
C(ethylene)–N(amine)–C(ethylene)	109.72(13)	109.73(13)

^aThe ligand located at the *trans* position toward the amine nitrogen atom. ^bLigands located at the *cis* position toward the amine nitrogen atom. Ligands located at the *trans* position toward the NO ligand.

performed under diamagnetic and paramagnetic conditions. The calculated geometry of the diamagnetic model agrees quite well with experimental results, while the Ru–N(amine nitrogen) length is considerably longer (3.0129 Å) in the paramagnetic model (Ru(IV)-carbanion) as shown in Figure S23, Supporting Information. Calculations predicted that occupied orbitals around the HOMO were principally contributed by $d\pi(\text{Ru})$ and $p(\text{Cl})$ orbitals, and three $d\pi(\text{Ru})$ orbitals were lying within the 1 eV region below the HOMO as shown in Figure S24, Supporting Information. These results indicated that the (iminium ion)ruthenium(II) was more reasonable model than (amine-carbanion)ruthenium(IV). The results of the X-ray analysis, NMR spectroscopy, and computational study suggested the diamagnetic model, a multiple bond between the N and the C atoms, and interactions between the Ru center and both N and C atoms.

Figure 9. Structure of $[\text{Ru}^{\text{II}}(\text{N}_3)_2\{\text{N}(\text{O})\text{CH}(\text{py})\text{CH}_2\text{N}(\text{C}_2\text{H}_5)\text{C}_2\text{H}_4\text{py}\}]$ ([8]).Figure 10. Structure of $[\text{Ru}^{\text{II}}\text{Cl}_2\{\text{N}(\text{O})\text{CH}(\text{py})\text{CH}_2\text{N}(\text{C}_2\text{H}_5)\text{C}_2\text{H}_4\text{py}\}]$ ([9]).

An alternative C–H activation reaction of the arm –CH₂– moiety next to the pyridyl group occurred in reactions of nitrosyl-ruthenium complexes, *fac*- and *mer*- $[\text{RuXY}(\text{NO})(\text{ebpea})]^+$, with N₃[–] in methanol affording a nitroso complex of ruthenium(II) having two azides as ancillary ligands, $[\text{Ru}^{\text{II}}(\text{N}_3)_2\{\text{N}(\text{O})\text{CH}(\text{py})\text{CH}_2\text{N}(\text{C}_2\text{H}_5)\text{C}_2\text{H}_4\text{py}\}]$ ([8]), in yields of 56–90%. The diazido-nitroso complex, [8], reacted with hydrochloric acid under refluxing conditions to change into a dichloronitroso complex substituted of azido ligands by chloride ions, $[\text{Ru}^{\text{II}}\text{Cl}_2\{\text{N}(\text{O})\text{CH}(\text{py})\text{CH}_2\text{N}(\text{C}_2\text{H}_5)\text{C}_2\text{H}_4\text{py}\}]$ ([9]). Selected structural parameters and structures of these nitroso complexes are summarized in Table 7 and shown in Figures 9 and 10. The structures of [8] revealed a distorted octahedral arrangement with six nitrogen atoms to the ruthenium(II) center. Structure parameters of the nitroso moieties, N1–O1, N1–C4, and Ru–N1–O1 were 1.2504(19) Å, 1.514(2) Å, and 136.71(12)° for [8] and 1.244(2) Å, 1.516(2) Å, and 135.98(11)° for [9], indicating formation of the bond between the nitrosyl and the deprotonated methylene group of the ethylene arm.

The ¹H NMR spectra of these nitroso complexes in CD₃NO₂ showed diamagnetic properties. The doublet signal of the –N(O)–CH– moieties at 6.19 ppm for [8] and 6.23 ppm for [9] and eight signals of two pyridine rings were nonequivalently observed. A characteristic N=O stretching vibration band in IR spectra was observed at 1408 and 1415 cm^{–1}, respectively. The cyclic voltammograms of the nitrosoruthenium(II) complexes showed irreversible oxidation and reduction waves as shown in Figure S17, Supporting Information. The controlled potential electrolysis of [9] at the potential of one-electron oxidation afforded a nitrosyl complex, which showed the typical electrochemical behavior of the {RuNO}^{6–1}-type complex and a characteristic NO stretching mode at 1885 cm^{–1} as shown in Figures S21 and S22, Supporting Information, respectively.

These results indicated that the redox waves were assigned to reduction and oxidation of the Ru–nitroso moiety. Reaction of *mer*-[RuCl(CH₃O)(NO)(ebpea)]PF₆ with NaOH gave a mixture of a nitro ruthenium(II) complex and the starting complex, while reaction of NaOCH₃ or NaN₃ afforded the nitroso complex. Although the nitro ruthenium complex was not obtained as a pure form, it was tentatively identified as [Ru^{II}(H₂O)(CH₃O)(NO₂)(ebpea)] by characteristic IR bands ($\nu(\text{NO}_2)$, 1415 and 1448 cm⁻¹), FAB MS (453, [Ru(H₂O)(CH₃O)(NO₂)(ebpea)] + H⁺; 435, [Ru(CH₃O)(NO₂)(ebpea)] + H⁺), and CV (irreversible oxidation wave of Ru(III)/Ru(II)). Electrochemical reduction reactions of *mer*-[RuCl₂(NO)(ebpea)]PF₆ (*mer*-[4]-PF₆) were performed at the potential of the one-electron reduction of *mer*-[4]PF₆ in CH₃CN by controlled potential electrolysis containing Et₄NClO₄ and the OTTLE (optically transparent thin-layer electrode) experiment containing Et₄NCl. The nitroso complex, [Ru^{II}Cl₂{N(O)CH(py)CH₂N(C₂H₅)C₂H₄py}] ([9]), was formed during electrochemical one-electron reduction. The CV showed the Ru(III)/Ru(II) oxidation potential, and the UV–vis spectrum showed a characteristic absorption band of the nitroso complex, [9] at 362 nm as shown Figures S19 and S20, Supporting Information. During reaction of *mer*-[RuCl(OH)(NO)(ebpea)]PF₆ with NaN₃ in CH₃OH under stirring for 24 h, H₂ evolution was confirmed by GC. We concluded that formation of the nitroso complexes occurred via one-electron reduction of the RuNO moiety followed by H abstraction from the alkyl arm. Detailed studies on formation of the nitroso complex are in progress by reduction of the nitrosyl complexes and reaction with nucleophiles.

CONCLUSIONS

Ethylbis(2-pyridylethyl)amine (ebpea) can coordinate to the ruthenium center in both the facial and the meridional fashion due to its flexible ethylene arms between the central amine and two pyridyl groups. The ebpea ligand was more flexible and had more reactive alkyl arms compared with the similar tridentate ethylbis(2-pyridylmethyl)amine (ebpma) ligand, having shorter methylene arms instead of the ethylene arms. Although coordination of the ebpma ligand in the meridional fashion was more structurally distorted than that in the facial fashion, the ebpea ligand coordinated to the ruthenium in the meridional as well as the facial fashion. Two π -acid pyridyl rings of the meridional complexes were situated in the trans position each other, and dihedral angles between the pyridyl rings were larger values than those of the ebpma complexes to share the different $d\pi(\text{Ru})$ orbitals. The characteristic ligand-base reactions of the ebpea complexes were found. Two different types of C–H activation reactions occurred at the ethylene arm of the ebpea ligand to afford (η^2 -iminium ion)ruthenium and nitrosoruthenium complexes having C–H bond activated ligands coordinated in a meridional fashion. The geometry of the complex is important for the interaction between the Ru center and the C–H bond of the ebpea ligand. These characteristics arise from the flexibility of the ethylene arm of the ebpea to stabilize a meridional coordination mode and convert between facial and meridional modes.

ASSOCIATED CONTENT

S Supporting Information. Characterization data, DFT calculation, and crystallographic information (CIF). This material is available free of charge via the Internet at <http://pubs.acs.org>.

AUTHOR INFORMATION

Corresponding Author

*E-mail: h-nagao@sophia.ac.jp.

ACKNOWLEDGMENT

The authors are grateful to Professor Koji Tanaka and Professor Tohru Wada for several measurements and their discussions.

REFERENCES

- (1) (a) Medlycott, E. A.; Hanan, G. S. *Coord. Chem. Rev.* **2006**, *250*, 1763. (b) Inglez, S. D.; Lima, F. C. A.; Silva, A. B. F.; Simioni, A. R.; Tedesco, A. C.; Daniel, J. F. S.; Lima-Neto, B. S.; Carlos, R. M. *Inorg. Chem.* **2007**, *46*, 5744. (c) Stagni, S.; Orselli, E.; Palazzi, A.; Cola, L. D.; Zacchini, S.; Femoni, C.; Marcaccio, M.; Paolucci, F.; Zanarini, S. *Inorg. Chem.* **2007**, *46*, 9126. (d) Abrahamsson, M.; Hammarstrom, L.; Tocher, D. A.; Nag, S.; Datta, D. *Inorg. Chem.* **2006**, *45*, 9580. (e) Bokach, N. A.; Haukka, M.; Hirva, P.; Guedes Da Silva, M. F. C.; Kukushkin, V. Y.; Pombeiro, A. J. L. *J. Organomet. Chem.* **2006**, *691*, 2368.
- (2) (a) Cooke, M. W.; Hanan, G. S.; Loiseau, F.; Campagna, S.; Watanabe, M.; Tanaka, Y. *J. Am. Chem. Soc.* **2007**, *129*, 10479. (b) Tannai, H.; Koizumi, T.; Wada, T.; Tanaka, K. *Angew. Chem., Int. Ed.* **2007**, *46*, 7112. (c) Polyansky, D.; Cabelli, D.; Muckerman, J. T.; Fujita, E.; Koizumi, T.; Fukushima, T.; Wada, T.; Tanaka, K. *Angew. Chem., Int. Ed.* **2007**, *46*, 4169. (d) Singh, P.; Fiedler, J.; Zalis, S.; Duboc, C.; Niemeyer, M.; Lissner, F.; Schleid, T.; Kaim, W. *Inorg. Chem.* **2007**, *46*, 9254. (e) Deshpande, M. S.; Kumbhar, A. A.; Kumbhar, A. S. *Inorg. Chem.* **2007**, *46*, 5450. (f) Fabre, M.; Jaud, J.; Hliwa, M.; Launay, J.-P.; Bonvoisin, J. *Inorg. Chem.* **2006**, *45*, 9332. (g) Wada, T.; Yamanaka, M.; Fujihara, T.; Miyazato, Y.; Tanaka, K. *Inorg. Chem.* **2006**, *45*, 8887.
- (3) (a) Gunanathan, C.; Ben-David, T.; Milstein, D. *Science* **2007**, *317*, 790. (b) Zhang, J.; Leitus, G.; Ben-David, T.; Mikstein, D. *Angew. Chem., Int. Ed.* **2006**, *45*, 1113. (c) Khaskin, E.; Iron, M. A.; Shimon, L. J. W.; Zhang, J.; Milstein, D. *J. Am. Chem. Soc.* **2010**, *132*, 8542. (d) Yang, X.; Hall, M. B. *J. Am. Chem. Soc.* **2010**, *132*, 120. (e) Tanaka, R.; Yamashita, M.; Nozaki, K. *J. Am. Chem. Soc.* **2009**, *131*, 14168. (f) Li, J.; Shiota, Y.; Yoshizawa, K. *J. Am. Chem. Soc.* **2009**, *131*, 13584. (g) Zhang, J.; Leitus, G.; Ben-David, Y.; Milstein, D. *J. Am. Chem. Soc.* **2005**, *127*, 10840. (h) Vlught, J. I.; Siegler, M. A.; Janssen, M.; Vogt, D.; Spek, A. L. *Organometallics* **2010**, *28*, 7025. (i) Friedrich, A.; Drees, M.; Kass, M.; Herdtweck, E.; Schneider, S. *Inorg. Chem.* **2010**, *49*, 5482.
- (4) (a) Mola, J.; Rodriguez, M.; Romero, I.; Lobet, A.; Parella, T.; Pater, A.; Duran, M.; Sola, M.; Benet-Bunchholz, J. *Inorg. Chem.* **2006**, *45*, 10520. (b) Serrano, I.; Rodriguez, M.; Romero, I.; Lobet, A.; Parella, T.; Campelo, J. M.; Luna, D.; Marinas, J. M.; Benet-Bunchholz, J. *Inorg. Chem.* **2006**, *45*, 2644. (c) Rodriguez, M.; Romero, I.; Lobet, A.; Deronzier, A.; Biner, M.; Parella, T.; Stoekli-Evans, H. *Inorg. Chem.* **2001**, *40*, 4150. (d) Romero, I.; Rodriguez, M.; Lobet, A.; Collomb-Dunand-Sauthier, M.-N.; Deronzier, A.; Parella, T.; Stoekli-Evans, H. *J. Chem. Soc., Dalton Trans.* **2000**, 1689.
- (5) Shimizu, Y.; Fukui, S.; Oi, T.; Nagao, H. *Bull. Chem. Soc. Jpn.* **2008**, *81*, 1285.
- (6) Part of this work has been reported as a communication: Fukui, S.; Suzuki, N.; Wada, T.; Tanaka, K.; Nagao, H. *Organometallics* **2010**, *29*, 1534.
- (7) Goto, M.; Koga, N.; Ohse, Y.; Kudoh, Y.; Kukihara, M.; Okuno, Y.; Kurosaki, H. *Inorg. Chem.* **2004**, *43*, 5120.
- (8) Fletcher, J. M.; Jenkins, I. L.; Lever, F. M.; Martin, F. S.; Powell, A. R.; Todd, R. *J. Inorg. Nucl. Chem.* **1955**, *1*, 378.
- (9) *Crystal Structure 3.6.0, Single Crystal Structure Analysis Software*; Molecular Structure Corp. and Rigaku Corp.: The Woodlands, TX and Rigaku: Tokyo, 2004.
- (10) Sheldrick, G. *SHELXL97: Program for Structure Refinement*; University of Göttingen, Germany, 1997.
- (11) Becke, A. D. *J. Chem. Phys.* **1993**, *98*, 5648.

(12) (a) Dunning, T. H., Jr.; Hay, P. J. In *Modern Theoretical Chemistry*; Schaefer, H. F., III, Ed.; Plenum: New York, 1976; pp 1–28. (b) Hay, P. J.; Wadt, W. R. *J. Chem. Phys.* **1985**, *82*, 270. (c) Wadt, W. R.; Hay, P. J. *J. Chem. Phys.* **1985**, *82*, 284. (d) Hay, P. J.; Wadt, W. R. *J. Chem. Phys.* **1985**, *82*, 299.

(13) Frisch, M. J.; Trucks, G. W.; Schlegel, H. B.; Scuseria, G. E.; Robb, M. A.; Cheeseman, J. R.; Montgomery, J. A., Jr.; Vreven, T.; Kudin, K. N.; Burant, J. C.; Millam, J. M.; Iyengar, S. S.; Tomasi, J.; Barone, V.; Mennucci, B.; Cossi, M.; Scalmani, G.; Rega, N.; Petersson, G. A.; Nakatsuji, H.; Hada, M.; Ehara, M.; Toyota, K.; Fukuda, R.; Hasegawa, J.; Ishida, M.; Nakajima, T.; Honda, Y.; Kitao, O.; Nakai, H.; Klene, M.; Li, X.; Knox, J. E.; Hratchian, H. P.; Cross, J. B.; Bakken, V.; Adamo, C.; Jaramillo, J.; Gomperts, R.; Stratmann, R. E.; Yazyev, O.; Austin, A. J.; Cammi, R.; Pomelli, C.; Ochterski, J. W.; Ayala, P. Y.; Morokuma, K.; Voth, G. A.; Salvador, P.; Dannenberg, J. J.; Zakrzewski, V. G.; Dapprich, S.; Daniels, A. D.; Strain, M. C.; Farkas, O.; Malick, D. K.; Rabuck, A. D.; Raghavachari, K.; Foresman, J. B.; Ortiz, J. V.; Cui, Q.; Baboul, A. G.; Clifford, S.; Cioslowski, J.; Stefanov, B. B.; Liu, G.; Liashenko, A.; Piskorz, P.; Komaromi, I.; Martin, R. L.; Fox, D. J.; Keith, T.; Al-Laham, M. A.; Peng, C. Y.; Nanayakkara, A.; Challacombe, M.; Gill, P. M. W.; Johnson, B.; Chen, W.; Wong, M. W.; Gonzalez, C.; Pople, J. A. *Gaussian 03*, Revision E.01; Gaussian, Inc.: Wallingford CT, 2004.

(14) (a) Mercer, E. E.; Dumas, P. E. *Inorg. Chem.* **1971**, *10*, 2755. (b) Gilbert, J. D.; Rose, D.; Wilkinson, G. *J. Chem. Soc. A* **1970**, 2765. (c) Rose, D.; Wilkinson, G. *J. Chem. Soc. A* **1970**, 1791.

(15) (a) Miranda, K. M.; Bu, X.; Lorkvic, I.; Ford, P. C. *Inorg. Chem.* **1997**, *36*, 4838. (b) Godwin, J. B.; Meyer, T. J. *Inorg. Chem.* **1971**, *10*, 471. (c) Drew, M. G. B.; Nag, S.; Datta, D. *Dalton Trans.* **2008**, 2298. (d) Caulton, K. G. *Coord. Chem. Rev.* **1975**, *14*, 317. (e) Richter-Addo, G. B.; Legdzins, P. *Metal Nitrosyls*; Oxford: New York, 1992.

(16) (a) Fukui, S.; Shimamura, Y.; Sunamoto, Y.; Abe, T.; Hirano, T.; Oi, T.; Nagao, H. *Polyhedron* **2007**, *26*, 4645. (b) Nagao, H.; Enomoto, K.; Wakabayashi, Y.; Komiya, G.; Hirano, T.; Oi, T. *Inorg. Chem.* **2007**, *46*, 1431. (c) Hirano, T.; Ueda, K.; Mukaida, M.; Nagao, H.; Oi, T. *J. Chem. Soc., Dalton Trans.* **2001**, 2341.

(17) (a) Chan, K.-W.; Huang, E. K.; Williams, I. D.; Leung, W.-H. *Organometallics* **2009**, *28*, 5794. (b) Singh, P.; Sieger, M.; Fiedler, J.; Su, C.-Y.; Kaim, W. *Dalton Trans.* **2008**, 868. (c) Videla, M.; Jacinto, J. S.; Baggio, R.; Garland, M. T.; Singh, P.; Kaim, W.; Slep, L. D.; Olabe, J. A. *Inorg. Chem.* **2006**, *45*, 8608. (d) Sarkar, S.; Sarkar, B.; Chanda, N.; Kar, S.; Mobin, S. M.; Fiedler, J.; Kaim, W.; Lahiri, G. K. *Inorg. Chem.* **2005**, *44*, 6092. (e) Chanda, N.; Paul, D.; Kar, S.; Mobin, S. M.; Datta, A.; Puranik, V. G.; Rao, K. K.; Lahiri, G. K. *Inorg. Chem.* **2005**, *44*, 3499. (f) Ferlay, S.; Schmalle, H. W.; Francese, G.; Stoeckli-Evans, H.; Imlau, M.; Schaniel, D.; Woike, T. *Inorg. Chem.* **2004**, *43*, 3500. (g) Chanda, N.; Mobin, S. M.; Puranik, V. G.; Datta, A.; Niemeyer, M.; Lahiri, G. K. *Inorg. Chem.* **2004**, *43*, 1056. (h) Hadadzadeh, H.; DeRosa, M. C.; Yap, G. P. A.; Rezvani, A. R.; Crutchley, R. J. *Inorg. Chem.* **2002**, *41*, 6521.